JOURNAL OF SOLID STATE CHEMISTRY 119, 191–196 (1995)

The Crystal Structure of Lanthanum Manganate(III), $LaMnO_3$, at Room Temperature and at 1273 K under N_2

P. Norby,[1] I. G. Krogh Andersen, and E. Krogh Andersen

Department of Chemistry, University of Odense, DK-5230 Odense M, Denmark

and

N. H. Andersen

Department of Solid State Physics, Risø National Laboratory, DK-4000 Roskilde, Denmark

Received February 24, 1995; in revised form May 18, 1995; accepted May 19, 1995

Orthorhombic stoichiometric $LaMnO_3$ is prepared by heating rhombohedral $LaMnO_{3+\delta}$ under N_2 at 1173 K and cooling to room temperature under N_2. The thermal transformations of orthorhombic lanthanum manganate(III) were investigated using high-temperature X-ray powder diffraction. Transformations orthorhombic–cubic–rhombohedral were observed. The dependence of the unit cell parameters on temperature was determined. The crystal structures of $LaMnO_3$ at room temperature (orthorhombic) and at high temperature (rhombohedral at 1273 K in N_2) were determined using neutron powder diffraction. © 1995 Academic Press, Inc.

INTRODUCTION

Lanthanum manganates(III)(IV) have attracted attention as cathode materials for high temperature solid oxide fuel cells (SOFC). Especially materials doped with Sr or Ca show promising properties. Detailed knowledge of the structure and the defect distribution is of interest in order to understand the oxygen ion transport mechanisms. Solid oxide fuel cells will be operating at temperatures of 1173–1273 K. It is therefore of considerable interest to know the crystal structure under actual working conditions.

Lanthanum strontium manganates(III)(IV), $La_{1-x}Sr_xMnO_{3+\delta}$, have distorted perovskite-type structures. The distortion depends on the actual stoichiometry (oxygen content and the La/Sr ratio) and is sensitive to the method of preparation and the oxygen partial pressure. In the present work materials without strontium are studied. Their composition will be given as $LaMnO_{3+\delta}$, assuming a La : Mn ratio of 1. Such materials prepared in air have rhombohedral structures and excess oxygen, or rather cation vacancies (1). Structural studies of rhombohedral lanthanum manganates(III)(IV) (2–4) as well as chemical analyses and density measurements (1) have shown that there is no interstitial oxygen. The oxygen lattice is fully occupied while cation vacancies are present, so that the crystallographic correct composition is $La_zMn_zO_3$, where $z = 3/(3 + \delta)$. For $\delta > 0$ manganese is present in oxidation states III and IV.

Lanthanum manganate(III) $LaMnO_3$, e.g., obtained by heating at 1173 K under N_2, is orthorhombic at room temperature (1). The structure has been investigated by Gilleo (5) and by Elemans *et al.* (6). In this work we have studied temperature-induced phase transitions and the crystal structure of $LaMnO_3$ at room temperature and at 1273 K under N_2. Two phase transformations are observed when lanthanum manganate(III). is heated. The high-temperature phase is rhombohedral and an intermediate cubic phase exists.

This work is part of a study of the structural phase diagram of lanthanum manganates(III)(IV) and Sr-substituted lanthanum manganates(III)(IV). A detailed study of chemical and structural properties of Sr-substituted lanthanum manganates(III)(IV) has been published in Ref. (1). Further studies concerning the structural dependence of temperature, oxygen partial pressure, and Sr substitution are in progress.

EXPERIMENTAL

The rhombohedral phase $LaMnO_{3+\delta}$ was prepared from acetates by solid state reaction and was calcined in air at 1373 K. The orthorhombic phase was prepared by heating the rhombohedral phase under a nitrogen flow at 1173 K.

[1] To whom correspondence should be addressed at present address: Chemistry Department, Brookhaven National Laboratory, Upton, NY 11973.

0022-4596/95 $12.00

Further details concerning the preparation procedure are given in Ref. (1).

By chemical analysis (determination of mean oxidation state of manganese and total manganese content (1)) the compositions of the materials were determined (normalized with respect to La);

Rhombohedral phase $La_{1.00}Mn^{III}_{0.72}Mn^{IV}_{0.28}O_{3.14}$
Orthorhombic phase $La_{1.00}Mn^{III}_{0.99}Mn^{IV}_{0.01}O_{3.005}$.

The material was characterized by X-ray powder diffraction at room temperature using a Siemens D5000 powder diffractometer equipped with a primary germanium monochromator giving Cu$K\alpha_1$ radiation (λ = 1.5405981 Å). Fluorescence radiation from manganese was reduced with energy discrimination using the technique described in Ref. (7). Unit cell parameters were refined from the X-ray data using the program CELLKANT (8).

High-temperature X-ray powder diffraction was performed with a Guinier Simon camera up to 1273 K using Cu$K\alpha_1$ radiation. The movement of the film cassette was synchronized with the temperature, making phase transitions visible. The sample was contained in a quartz glass capillary and heated by a flow of hot nitrogen.

High-temperature synchrotron powder diffraction data of the orthorhombic lanthanum manganate(III) were collected at NSLS, Brookhaven National Laboratory, using the instrument X7B equipped with a position-sensitive detector (120° INEL CPS120). The wavelength was 1.4898 Å. The sample was kept in a quartz glass capillary and data were collected from room temperature up to 920 K. Unit cell parameters were determined using the profile-fitting program ALLHKL (9).

Neutron powder diffraction experiments were performed at Risø National Laboratory, Denmark. In order to increase the amount of material in the beam the materials were pressed into pellets. For the room temperature measurements the pellets were mounted on an aluminum stand and wrapped in vanadium foil. Room-temperature data were collected using a wavelength of 1.0777 Å from 10 to 116° in 2θ, step length 0.053°.

High-temperature neutron powder diffraction data were collected with the samples contained in a quartz tube under a flow of N_2. The evacuated furnace was heated by a tantalum foil filament. High temperature data were collected using a wavelength of 1.4792 Å from 20 to 126 in 2θ, step length 0.053°.

The program ALLHKL (9) was used for profile fitting, and DBW3.2S (10) was used for Rietveld refinement.

RESULTS

Room Temperature Structure

The room-temperature X-ray powder diffraction pattern could be indexed based on an orthorhombic unit cell: a = 5.7046(2), b = 7.7029(4), and c = 5.5353(3) Å. Systematic extinctions were in agreement with the space group *Pnma*, in accordance with the findings in Ref (6).

Neutron powder diffraction data were used for the structure refinement. In order to determine small deviations from stoichiometry, especially oxygen contents, it is necessary to use neutron data and to include data at high $\sin(\theta)/\lambda$. When X-ray radiation is used, the heavier elements dominate due to their high scattering power, whereas oxygen has a high scattering length for neutrons.

TABLE 1
Structural Data for the Neutron Powder Diffraction Study of $LaMnO_3$ at Room Temperature

	x	y	z	B	n	ν
La	0.5435(5)	0.25	0.0063(7)	0.3(1)	0.99(3)	2.9
Mn	0	0	0	0.2(1)	1	3.1
O1	−0.0107(8)	0.25	−0.0733(8)	0.6(1)	1.06(4)	2.1
O2	0.3014(5)	0.0385(4)	0.2257(6)	0.5(1)	1.97(6)	2.0

Mn-O1	1.973(1) ×2	Mn-O2	1.918(6) ×2	
Mn-O2*	2.145(5) ×2			
O1-Mn-O2	90.4(8) ×2	89.6(8) ×2	O1-Mn-O1	180
O1-Mn-O2*	90.5(8) ×2	89.5(8) ×2	O2-Mn-O2	180
O2-Mn-O2*	90.6(2) ×2	89.4(2) ×2	02*-Mn-O2*	180
Mn-O1-Mn	156.0(3)		Mn-O2-Mn	156(1)
La-O1	2.418(6)	2.579(5)	3.156(6)	3.189(5)
La-O2	2.46(2) ×2	2.65(2) ×2	2.72(3) ×2	3.35(2) ×2

Orthorhombic *Pnma*, a = 5.6991(7), b = 7.7175(9), and c = 5.5392(6) Å. Final R values: R_p: 7.6, R_{WP}: 9.7, S: 1.3.

Note: Refined atomic coordinates, isotropic temperature factors B (Å^2), population factors n, and bond valence ν (Ref. 12). Distances (Å) and angles (°). Standard deviations in parentheses.

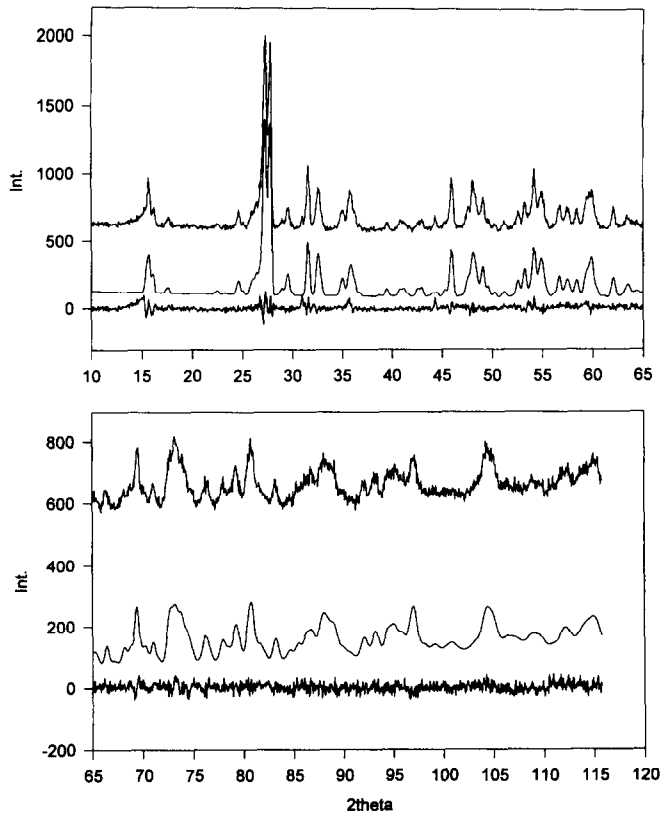

FIG. 1. Observed, calculated, and difference neutron powder diffraction profiles for $LaMnO_3$ at room temperature (orthorhombic).

As starting parameters for the Rietveld refinement coordinates from Ref. (6) were used. Fifteen structural and ten profile parameters were refined using a pseudo-Voigt peak shape. Population parameters for all atoms except manganese were varied. The refinement converged at an R_{wp} value of 9.7%. The refined parameters are listed in Table 1. Interatomic distances and angles are also given in this table. Observed, calculated, and difference diagrams are shown in Fig. 1. Data up to $\sin(\theta)/\lambda = 0.72$ were included in the refinement.

The refined structure is in agreement with chemical analyses, showing the compound to be almost stoichiometric. In evaluating population parameters it is necessary to consider the very high correlation between temperature factors and population parameters, as demonstrated in a recent paper (4). The small wavelength used is favorable in simultaneous refining of temperature factors and population parameters in nonstoichiometric compounds. Whereas the rhombohedral lanthanum manganate(III)(IV) at room temperature has a fully occupied oxygen lattice with vacancies at lanthanum and manganese positions, the refinement of the orthorhombic phase indicates that the populations of La, Mn, and O are equal.

Thermal Transformation

When orthorhombic lanthanum manganate(III) is heated, two phase transitions are visible at the Guinier–Simon film below 1273 K. At ca. 600 K a transformation to a cubic phase is observed (a = 7.846(1) Å). In comparison to the unit cell of the ideal cubic perovskite, the axes have been doubled. Upon further heating a phase transition to a rhombohedral phase occurs at ca. 800 K. The unit cell dimensions at 1273 K were found from the Guinier–Simon film to be a = 5.545(1) and c = 6.733(2) Å (hexagonal setting). These values deviate slightly from the values determined from the high-temperature neutron powder diffraction experiment (see below). The reason is that no internal standard was used in the Guinier–Simon experiment. From the synchrotron high-temperature experiments it was evident that the c axis was doubled, giving unit cell dimensions similar to those of the low-temperature rhombohedral $LaMnO_{3+\delta}$. A thermally induced transformation from orthorhombic to cubic symmetry for $LaMnO_3$ was observed by Iserentant *et al.* (11), although at a lower temperature (523 K).

The refined unit cell parameters and volumes determined from the synchrotron powder diffractograms by profile refinement are shown in Fig. 2. To facilitate com-

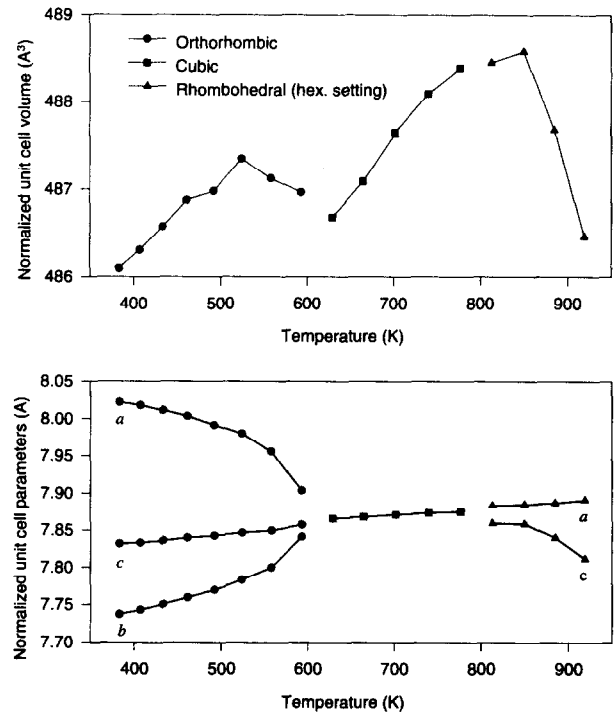

FIG. 2. Unit cell parameters as a function of temperature when orthorhombic $LaMnO_3$ is heated from room temperature to 920 K. Unit cell parameters were determined by profile refinement using the program ALLHKL (9). In order to compare the unit cells for the different phases the unit cell axes were transformed into psuedo-cubic axes.

TABLE 2
Relations between Unit Cell Parameters in Distorted Perovskites

	a	b	c	Volume
"Ideal" cubic perovskite	a			a^3
Orthorhombic distortion	$\sim\sqrt{2}a$	$\sim 2a$	$\sim\sqrt{2}a$	$\sim 4a^3$
"Cubic distortion"	$\sim 2a$			$\sim 8a^3$
Trigonal distortion	a	c	α	Volume
Hexagonal setting	$\sim\sqrt{2}a$	$\sim 2\sqrt{3}a$		$\sim 6a^3$
Rhombohedral setting	$\sim\sqrt{2}a$		$\sim 60°$	$\sim 2a^3$

The ideal perovskite is cubic with unit cell parameter a.

parison between unit cell dimensions, the unit cell parameters have been transformed to a common pseudo-cubic scale by transformation to magnitudes comparable with those of the observed cubic phase. The relations between the unit cells of the orthorhombic, cubic, and rhombohedral phases are given in Table 2.

Figure 2 shows that as the material is heated the difference between the orthorhombic a and c axes decreases, and they merge at the transition to the cubic phase. The volume of the orthorhombic unit cell shows normal thermal expansion until close to the orthorhombic–cubic transformation, where a decrease in unit cell volume is observed. The cubic phase shows again normal thermal expansion, which continues across the cubic–rhombohedral phase transition. Upon further heating, the unit cell volume decreases, mainly determined by a decrease in the c axis (hexagonal setting). This decrease is due to oxidation of the material, caused by diffusion of air into the capillary, leading to a shortening of the Mn—O bonds.

TABLE 3
Structural Data for the Neutron Powder Diffraction Study of Rhombohedral $LaMnO_3$ at 1273 K in N_2

	x	y	z	B	n
La	0	0	0.25	2.5(2)	1.00(5)
Mn	0	0	0	1.4(3)	1
O	0.4463(7)	0	0	3.4(1)	3.0(2)

Mn–O	2.000(1) ×6		
O–Mn–O	91.0(1) ×6	89.0(1) ×6	180 ×3
Mn–O–Mn	162.7(2)		
La–O	2.504(4)×3	2.805(1) ×6	3.107(4) ×3

Hexagonal setting ($R\bar{3}c$), a = 5.6109(5), c = 13.619(1) Å. Final R values: R_p: 7.8, R_{WP}: 9.9, S: 1.4.

Note: Refined atomic coordinates, isotropic temperature factors B (Å^2), and population factor n. Distances (Å) and angles (°). Standard deviations in parentheses.

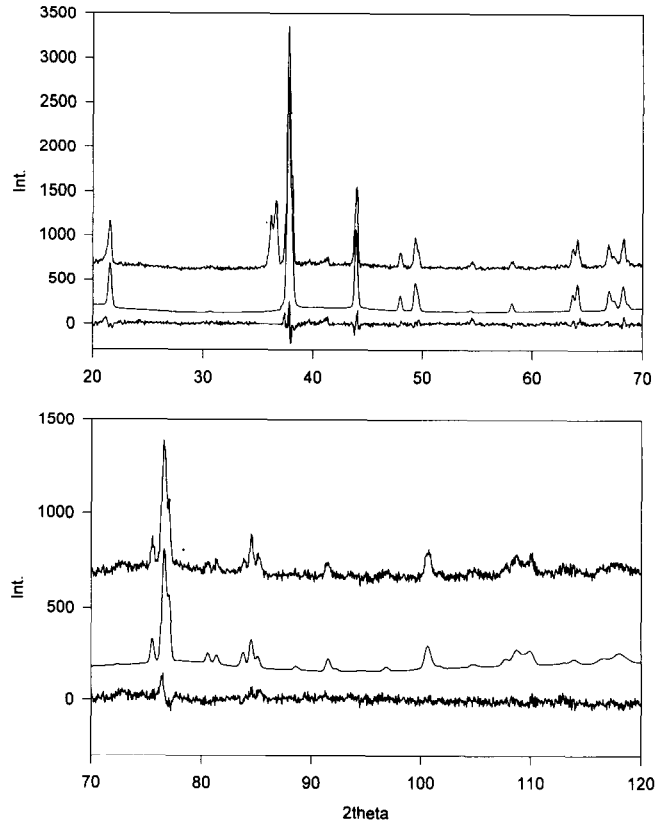

FIG. 3. Observed, calculated, and difference neutron powder diffraction profiles for $LaMnO_3$ at 1273 K in N_2 (rhombohedral).

High-Temperature Structure

The high-temperature neutron powder diagram was fitted using the profile-fitting program ALLHKL (9). Good agreement between observed and calculated patterns was obtained using the space group $R\bar{3}c$. The refined unit cell parameters from the neutron data were a = 5.6109(5) and c = 13.619(1) Å. As starting parameters for the Rietveld refinement DBW3.2S (10), coordinates from Ref. (4) were used. Population parameters were refined except for manganese. The refined parameters are given in Table 3 together with interatomic distances and angles. Observed, calculated, and difference profiles are shown in Fig. 3. Data from 35–37° in 2θ were excluded from the refinements because of reflections from the furnace.

The structure of the high-temperature rhombohedral phase is basically similar to the room temperature structure of the rhombohedral lanthanum manganate(III)(IV). Structure refinement of low-temperature rhombohedral lanthanum manganate(III)(IV) (e.g., $LaMnO_{3.16}$, Ref. 3) indicates a fully occupied oxygen lattice and defects on the cation sites. In the rhombohedral high-temperature lanthanum manganate(III) under N_2 the refinement indicates a fully occupied cation lattice in accordance with

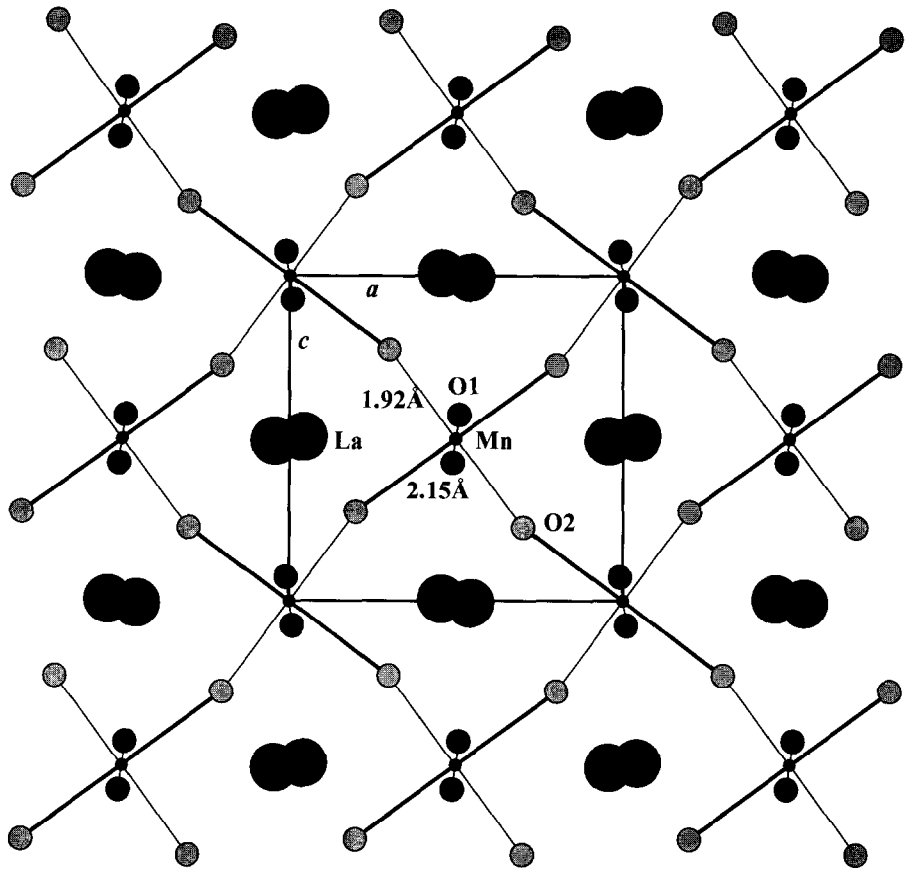

FIG. 4. Projection of the crystal structure of orthorhombic $LaMnO_3$ along the *b* axis.

the chemical composition. In the rhombohedral structure all Mn—O distances are equal. The MnO_6 octahedron is slightly angularly distorted as seen from Table 3. The oxygen coordination of lanthanum is more regular than for the orthorhombic phase.

DISCUSSION

The lowering of symmetry from the ideal cubic perovskite is due to two factors. In the ideal cubic perovskite the Mn—O—Mn angle is 180°. Lanthanum has 12 nearest oxygen neighbors at a distance of $a\sqrt{2}$. By lowering the symmetry to trigonal, the Mn—O—Mn angle is allowed to deviate from 180°, and lanthanum becomes irregularly 12-coordinated. The MnO_6 octahedra have equal Mn—O distances but are rotated around the threefold axis. Structure determinations have shown that the octahedra are almost regular. The Jahn–Teller distortion of the MnO_6 octahedra lowers the symmetry further to orthorhombic, where the Mn—O distances are allowed to vary.

In the orthorhombic room-temperature phase both chemical analyses and the structure refinement indicate a near-stoichiometric composition with an average oxidation state of 3 for manganese. Bond valence calculations (12) (Table 1) give reasonable values. The bond valence sum for Mn is 3.1 as opposed to the expected 3.0. However, considering the accuracy of especially the Mn—O2 distances, the discrepancy may not be significant.

The oxygen coordination around manganese may be seen as a distorted octahedron; see Table 1. The MnO_6 octahedra in the room temperature orthorhombic lanthanum manganate(III) are Jahn–Teller distorted as expected for Mn^{3+}, with two long Mn—O2 distances of 2.14 Å . However, the distortion in the 3-dimensional Mn—O framework is not a polar distortion, and the distorted octahedra do not have square planar baseplanes.

As seen from Table 1 the equatorial plane displays two significantly different Mn—O distances of 1.97 (O1) and 1.92 Å (O2). O1 has two manganese neighbors at the same distance (1.97 Å) and bonds the MnO_6 polyhedra together along the *b* axis. O2 has one short (1.92 Å) and one long (2.14 Å) Mn contact, giving a mean Mn—O2 distance of 2.02 Å. Figure 4 shows a projection of the orthorhombic structure along the *b* axis. The Mn—O1 bond (1.97 Å) is

directed approximately along [010]. As seen in Fig. 4 the directions of the Jahn–Teller distorted Mn—O bonds are not parallel. All the long Mn—O bonds lie in the (101) plane, but are directed approximately along [101] and [10$\bar{1}$] in an alternating fashion.

Only a few oxides containing Mn(III) have been structurally characterized. Jahn–Teller distortions in compounds with Mn—O—Mn contacts have been described for Mn_2O_3 (13), where one of the manganese atoms has Jahn–Teller distorted oxygen coordination. In $MnPO_4 H_2O$ (containing no Mn—O—Mn bonds) similar distortions are observed (14).

In connection with studies of structural aspects of strontium-substituted lanthanum manganate(III)(IV) we are especially interested in the defect distribution. By combining chemical analyses with detailed structural information we hope to elucidate the nature of the defects and shed some light on the oxygen ion transport mechanisms.

In the present work we have investigated the stoichiometric lanthanum manganate(III), $LaMnO_3$, at room temperature and at 1273 K under N_2. At higher temperatures phase transitions first to cubic and then to rhombohedral are observed. The phase transitions are not accompanied by chemical changes (e.g., changes in oxygen stoichiometry), and in agreement with this the structure refinements show fully occupied oxygen lattices. The Jahn–Teller distortion of the MnO_6 octahedra found in the orthorhombic room-temperature phase is not seen in the high-temperature rhombohedral phase, where all Mn—O distances are (crystallographically) equal.

ACKNOWLEDGMENTS

This work has been supported by the Danish Ministry of Energy, ELSAM, ELKRAFT (DK-SOFC 1990–1992), and by the ALBANI Brewery Foundation. We thank Dr. J. C. Hanson, Brookhaven National Laboratory, for help with the synchrotron experiments (Contract DE-AC02-76CH00016 with the U.S. Dept. of Energy by its Division of Chemical Sciences, Office of Basic Energy Sciences).

REFERENCES

1. I. G. Krogh Andersen, E. Krogh Andersen, P. Norby, and E. Skou, *J. Solid State Chem.* **113,** 320 (1994).
2. B. C. Tofield and W. R. Scott, *J. Solid State Chem.* **10,** 183 (1974).
3. J. A. M. Van Roosmalen, "Some Thermochemical Properties of (La,Sr)$MnO_{3+\delta}$ as a Cathode Material for Solid State Oxide Fuel Cells" Thesis, Amsterdam University, Amsterdam, 1993.
4. S. Habekost, P. Norby, J. E. Jørgensen, and B. Lebech, *Acta Chem. Scand.* **48,** 337 (1994).
5. M. A. Gilleo, *Acta Crystallogr.* **10,** 161 (1957).
6. J. B. A. A. Elemans, B. Van Laar, K. R. Van Der Veen, and B. O. Loopstra, *J. Solid State Chem.* **3,** 238 (1971).
7. P. Norby, *J. Appl. Crystallogr.* **27,** 129 (1994).
8. N. O. Ersson, "Program CELLKANT," Institute of Chemistry, Uppsala University, Uppsala, Sweden, 1981.
9. G. S. Pawley, *J. Appl. Crystallogr.* **14,** 357 (1981).
10. D. B. Wiles and R. A. Young, *J. Appl. Crystallogr.* **14,** 149 (1981).
11. C. M. Iserentant, G. C. Robbrech, and H. M. Lippens, *Bull. Belg. Soc. Ser. V* **4/5,** 219 (1967).
12. I. D. Brown and D. Altermatt, *Acta Crystallogr. Sect. B* **41,** 244 (1985).
13. S. Geller, *Acta Crystallogr. Sect. B.* **27,** 821 (1971).
14. P. Lightfoot, A. K. Cheetham, and A. W. Sleight, *Inorg. Chem.* **26,** 3544 (1987).